Materials of the Conference
«PHYSICO-CHEMICAL FOUNDATIONS
OF METALLURGICAL PROCESSES"
named after Academician A.M. Samarin – 2022

По материалам конференции
«ФИЗИКО-ХИМИЧЕСКИЕ ОСНОВЫ
МЕТАЛЛУРГИЧЕСКИХ ПРОЦЕССОВ»
им. академика А.М. Самарина – 2022

UDC 669.187.2: 628.511/.512: 504.05
DOI 10.17073/0368-0797-2023-3-344-355

Original article
Оригинальная статья

Lead and zinc selective extraction from EAF dust while heating in resistance furnace with flowing argon

N. V. Podusovskaya [1, 2], O. A. Komolova [1, 2], K. V. Grigorovich [1, 2], A. V. Pavlov [2], V. V. Aksenova [2], B. A. Rumyantsev [1], M. V. Zheleznyi [1, 2]

[1] **Baikov Institute of Metallurgy and Materials Science, Russian Academy of Sciences** (49 Leninskii Ave., Moscow 119991, Russian Federation)
[2] **National University of Science and Technology "MISIS"** (4 Leninskii Ave., Moscow 119049, Russian Federation)

ndemidova_n@mail.ru

Abstract. The elemental and phase compositions of electric arc furnace (EAF) dust from PJSC Severstal were studied. We carried out the thermodynamic modeling of zinc and lead selective extraction process and determined its possible mechanisms. EAF dust was heated in the temperature range of 20 – 1300 °C in vacuum resistance furnace and the Tamman furnace with flowing argon. Experiments in the vacuum resistance furnace with linear heating showed that lead and zinc removal from the sample occurs in the temperature range of 800 – 1200 °C, with higher lead removal rate. Intensive lead removal was observed at temperature above 1000 °C, while intensive zinc removal occurs at temperature above 1200 °C. Clarifying isothermal experiments performed in the Tamman furnace showed that lead complete transition to the gas phase was achieved at a temperature of 1100 °C (holding time – 12 min) and at a temperature of 1200 °C (holding time – 6 min or more). At the same time, zinc removal was observed in the amount of 14.4 % ratio and 32.2 % ratio, respectively, which allows us to conclude that it is possible to consistently obtain two products: lead and zinc mixture and zinc not contaminated with lead. When comparing experimental and thermodynamic modeling data, the reactions that are most likely to occur during the carbon reduction of lead- and zinc-containing phases were determined.

Keywords: ferrous metallurgy, non-ferrous metals, steel dust, electric-arc furnace dust, EAF-dust, carbon-free process, selective extraction, evaporation, zinc, lead, iron, secondary resources, resource saving

For citation: Podusovskaya N.V., Komolova O.A., Grigorovich K.V., Pavlov A.V., Aksenova V.V., Rumyantsev B.A., Zheleznyi M.V. Lead and zinc selective extraction from EAF dust while heating in resistance furnace with flowing argon. *Izvestiya. Ferrous Metallurgy*. 2023;66(3):344–355. https://doi.org/10.17073/0368-0797-2023-3-344-355

Изучение селективного извлечения свинца и цинка из пыли ДСП при нагреве в печах сопротивления в токе аргона

Н. В. Подусовская [1, 2], О. А. Комолова [1, 2], К. В. Григорович [1, 2], А. В. Павлов [2], В. В. Аксенова [2], Б. А. Румянцев [1], М. В. Железный [1, 2]

[1] **Институт металлургии и материаловедения им. А.А. Байкова РАН** (Россия, 119991, Москва, Ленинский пр., 49)
[2] **Национальный исследовательский технологический университет «МИСИС»** (Россия, 119049, Москва, Ленинский пр., 4)

ndemidova_n@mail.ru

Аннотация. Изучены элементный и фазовый составы пыли дуговой сталеплавильной печи ПАО «Северсталь», проведено термодинамическое моделирование процесса селективного извлечения цинка и свинца из пыли. Определены возможные механизмы его протекания. Выполнен нагрев электросталеплавильной пыли в диапазоне температур 20 – 1300 °C в вакуумной печи сопротивления и печи Таммана в токе аргона.

Эксперименты в вакуумной печи сопротивления с линейным нагревом показали, что удаление свинца и цинка из образца протекало в интервале температур 800 – 1200 °С. При этом скорость удаления свинца была выше. Интенсивное удаление свинца наблюдали при температурах свыше 1000 °С, а интенсивное удаление цинка при температурах свыше 1200 °С. Уточняющие изотермические эксперименты, выполненные в печи Таммана, показали, что полный переход свинца в газовую фазу достигался при температуре 1100 °С (время выдержки 12 мин) и при температуре 1200 °С (время выдержки 6 мин и более). Параллельно с этим наблюдали удаление цинка в количестве 14,4 и 32,2 % (отн.) соответственно, что позволило сделать вывод о возможности последовательного получения двух продуктов: смеси свинца с цинком и цинка, не загрязненного свинцом. При сопоставлении экспериментальных данных и данных термодинамического моделирования определены реакции, протекание которых наиболее вероятно при восстановлении свинец- и цинксодержащих фаз углеродом.

Ключевые слова: черная металлургия, цветные металлы, сталеплавильная пыль, пыль ДСП, безуглеродный процесс, селективное извлечение, испарение, цинк, свинец, железо, вторичные ресурсы, ресурсосбережение

Для цитирования: Подусовская Н.В., Комолова О.А., Григорович К.В., Павлов А.В., Аксенова В.В., Румянцев Б.А., Железный М.В. Изучение селективного извлечения свинца и цинка из пыли ДСП при нагреве в печах сопротивления в токе аргона. *Известия вузов. Черная металлургия*. 2023;66(3):344–355. https://doi.org/10.17073/0368-0797-2023-3-344-355

Introduction

The accumulation of electric arc furnace (EAF) dust in the dumps of metallurgical companies contains significant amounts of zinc (typically 15 – 25 %) and lead (up to 3 %). Given the limited reserves of zinc and lead ores[1], as well as the low content of these metals in the dust, it has become crucial to develop technologies for the selective extraction of non-ferrous metals from EAF dust. Reprocessing this dust would not only allow for the recovery of zinc, lead, and iron for metallurgical production but also address the issue of toxic waste occupying substantial areas [1].

In general, zinc and lead in the EAF dust are present in the form of oxides due to the oxidizing nature of the steelmaking process. However, in the gas flow, there is a high probability of the formation of complex oxides, such as zinc ferrite $ZnFe_2O_4$ [2 – 4]. Moreover, the diverse chemical composition of materials processed in the EAF leads to variations in both the chemical and phase compositions of the EAF dust. This necessitates continuous monitoring when disposing of metallurgical dust and complicates EAF dust disposal procedure [5].

Currently, selective extraction of lead and zinc from the EAF dust is primarily carried out using hydrometallurgical methods [6; 7] or integrated pyro-hydrometallurgical methods [4; 8; 9]. However, the hydrometallurgical process is highly complex and involves multiple technological stages that require large amounts of chemical reagents, overheated vapor, hot water, and energy-intensive equipment. This poses environmental risks as numerous production sites are associated with poorly regulated or unregulated emissions of spent reagents, heat, energy carriers, production wastes and by-products [10; 11]. Therefore, it appears advisable to explore pyrometallurgical methods for the reprocessing of EAF dust to achieve selective extraction of lead and zinc.

An overview of studies on the disposal of toxic EAF dust reveals that the majority of efforts are focused on conventional approaches that utilize excessive amounts of reducing agents, such as carbon, to lower the starting temperature of zinc and other metals recovery. However, this hampers the selective extraction of these metals during the recovery process.

Furthermore, the reduction of industrial carbon consumption to mitigate CO_2 emissions has become a key objective for BRICS countries [12]. In Russia, specifically, government measures have been planned to address greenhouse gas emissions according to sources[2, 3]. These measures include:

– implementation of mandatory carbon accounting;

– establishment of performance targets for companies;

– implementation of fees or fines for excessive emissions;

– introduction of carbon emission trading;

– technological upgrades in production process.

These governmental actions impose restrictions on metallurgical technologies that are associated with significant greenhouse gas emissions. As a result, there is a need to develop methods for the selective extraction of lead and zinc from the EAF dust that do not rely on the use of additional reducing agent.

Object of research

The research focuses on the EAF dust from PJSC Severstal, which exhibits the following element composition (wt. %): 41.4 Fe; 14.5 Zn; 6.2 Ca; 2.5 Mn; 1.7 Cl; 1.74 C; 1.3 Si; 1.0 K; 1.0 Pb; 0.74 S; 0.2 Cr; 0.2 Cu; 0.1 Ti; with the remaining portion likely being oxygen. The determination of element content ranging from Na to U was performed using the MAX-GVM wave-dispersion *X*-ray fluorescent spectroscan specimen (MAX-GVM). This method involves exposing the sample to pri-

[1] Governmental report "On conditions and usage of raw mineral resources in the Russian Federation in 2020". URL: https://www.mnr.gov.ru/upload/iblock/74a/GD_msb-2020.pdf (access date 11.05.2023).

[2] Federal Law dated 02.07.2021 No. 296-ФЗ "On restriction of emissions of greenhouse gases". URL: http://publication.pravo.gov.ru/Document/View/0001202107020031 (access date 11.05.2023).

[3] Governmental decree of the Russian Federation dated October 29, 2021 No. № 3052-p. URL: http://publication.pravo.gov.ru/Document/View/0001202111010022 (access date 11.05.2023).

mary radiation from an *X*-ray tube, measuring the intensity of secondary fluorescent irradiation at wavelengths corresponding to the elements of interest, and subsequently calculating the weight fraction of these elements using fundamental parameter methods. Sample preparation involved milling and averaging loose samples, mixing them with a binder (polyacrylamide) at a concentration of 0.2 wt. % above the sample, wetting, forming the mixture into moderate-height cylinders (D = 7 mm, h = 2 – 3 mm), and drying. For solid samples, polished cross-sections were prepared.

The carbon and sulfur content was determined using a Leco CS 600 instrument through high temperature extraction in a carrier gas. The determination of carbon and sulfur involved combusting the sample in an oxygen flow (99.998 %) in the presence of special fluxes, followed by the measurement of the formed carbon dioxide (CO_2) and sulfur dioxide (SO_2).

The phase composition of the EAF dust was determined using *X*-ray diffraction (XRD). The phase content (wt. %) was found to be as follows: 78.2 Fe_3O_4; 4.4 $(Zn, Mn, Fe)_3O_4$; 6.0 ZnO; 4.5 $Ca_2Fe_2O_5$; 3.0 MnO_2; 2.7 Pb_2O_3; 1.2 SiO_2. It should be noted that since the structures of magnetite and spinel are essentially identical, they can be considered as a combined phase.

Theoretical objectives

Previous studies have suggested that selective reduction of lead from the EAF dust can be achieved with an insufficient amount of reducing agent. For example, it was demonstrated in [13] that during the reducing melting of lead agglomerate, selective reduction of lead can be achieved with a limited amount of carbon monoxide as a reducing agent (CO content not exceeding 60 %). Similar effects of solid carbon on the reduction of lead-containing industrial wastes were also considered in [14; 15]. It was observed that when the carbon content exceeded 3 %, combined reduction of lead and zinc from EAF dust occurred. Furthermore, when the carbon content exceeded 3.7 %, the selectivity of lead reduction from copper melting dust became more complex.

In order to determine the conditions necessary for the selective extraction of zinc and lead from EAF dust, it is crucial to identify the temperatures at which the zinc and lead compounds in the dust transition into the gas phase.

According to [16], HSC Chemistry 6 software has been successfully utilized to evaluate thermodynamic parameters, and the simulated results have shown good comparability with experimental data. The software employs calculating modules that rely on a comprehensive thermochemical database encompassing enthalpy (H), entropies (S), and reaction heat capacitances (C_p). By calculating changes in Gibbs energies, thermodynamic temperatures of reactions ($\Delta G < 0$) can be determined. The thermodynamic simulation considered reactions involving the reduction, thermal dissociation, and evaporation of detected lead and zinc-containing phases, as well as the reduction of iron and manganese oxides.

Table 1 summarizes the reduction of lead oxide (III) and the subsequent transition of lead and its compounds into the gas phase. The thermodynamic simulation assumed a carbon monoxide pressure of 1 atm.

From Table 1, it can be observed that the reduction of lead oxide (III) and the transition of lead into the gas phase begin at temperature not exceeding 877 °C.

Table 2 summarizes the reduction of zinc oxide and the accompanying transition of zinc into the gas phase.

According to Table 2, the reduction of zinc oxide with consideration for thermodynamics starts from the temperature exceeding 958 °C. However, it has been demonstrated in [17 – 19] that zinc reduction from EAF dust can occur successfully in the temperature range of 925 – 1300 °C with an excessive amount of reducing agent.

Reduction of complex spinel $(Zn, Mn, Fe)_3O_4$, specifically zinc ferrite $ZnFe_2O_4$ (franklinite), by carbon and carbon monoxide upon heating is investigated. The reactions of franklinite reduction which begin in the temperature range of 0 – 1326 °C are shown in Table 3.

Reactions 4 – 7, 10 – 12 in Table 3 exhibit similar starting temperatures for the reduction of lead and zinc-containing phases, emphasizing the need for accurate selection of temperature and composition of the gas phase to enable selective extraction of lead and zinc from EAF dust.

Since the spinel $(Zn, Mn, Fe)_3O_4$, detected in the EAF dust is not included in the HSC Chemistry 6 database,

Table 1

Lead (III) oxide reduction chemical reactions with their course temperatures, resulting in lead and its compounds transition into the gas phase

Таблица 1. **Химические реакции восстановления оксида свинца (III), сопровождающиеся переходом свинца и его соединений в газовую фазу, и температуры их протекания**

No.	Reaction	Reaction temperature, °C
1	$Pb_2O_3 + 3C = 2Pb_{(g)} + 3CO_{(g)}$	>449
2	$Pb_2O_3 + 1.5C = 2Pb_{(g)} + 1.5CO_{2(g)}$	>295
3	$Pb_2O_3 + 3CO_{(g)} = 2Pb_{(g)} + 3CO_{2(g)}$	0 – 2000
4	$Pb_2O_3 + C = 2PbO_{(g)} + CO_{(g)}$	>809
5	$2Pb_2O_3 + C = 4PbO_{(g)} + CO_{2(g)}$	>835
6	$Pb_2O_3 + CO_{(g)} = 2PbO_{(g)} + CO_{2(g)}$	>877

Table 2

Zinc oxide reduction chemical reactions with their course temperatures, resulting in zinc transition into the gas phase

Таблица 2. **Химические реакции восстановления оксида цинка, сопровождающиеся переходом цинка в газовую фазу, и температуры их протекания**

No.	Reaction	Reaction temperature, °C
7	$ZnO + C = Zn_{(g)} + CO_{(g)}$	>958
8	$2ZnO + C = 2Zn_{(g)} + CO_{2(g)}$	>1064
9	$ZnO + CO_{(g)} = Zn_{(g)} + CO_{2(g)}$	>1326

possible reduction reactions were considered for the compounds iron or manganese oxides (Fe_3O_4 and Mn_3O_4). The reactions, which occur in the temperature range of 295 – 1400 °C, are summarized in Table 4.

In accordance with Table 4, reactions 15 – 25 can occur simultaneously with the reduction of lead oxide (III).

Since the transition of zinc-containing phases into gas phase will occur after the reduction of lead (and possibly other components of EAF dust), it is likely that the carbon present in the dust will be fully consumed for other components. Therefore, without an additional reducing agent, the mechanism for the transition of zinc into the gas phase will be the thermal dissociation of zinc oxide (as shown in Table 5).

The temperature required for reaction 26 is too high for industrial conditions. The starting temperature of thermal dissociation can be reduced by decreasing the partial pressure of the resulting gases through the addition of argon. In order to confirm this, a thermodynamical simulation of the equilibrium composition was performed for the reaction of thermal decomposition of zinc oxide using Terra software [20]. The temperature of reaction $ZnO = Zn_{(g)} + O_{2(g)}$ as a function of the partial pressure of $Zn_{(g)}$ is illustrated in Fig. 1.

From Fig. 1, it can be observed that a decrease in the partial pressure of $Zn_{(g)}$ (by argon addition) would allow for a reduction in the temperature range of thermal decomposition of zinc oxide from 1970 to 1300 °C.

Theoretically, a similar approach can be applied to reduce the starting temperature of the reduction of lead oxide (III) in order to expand the range of selective extraction of lead and zinc-containing phases.

It has been determined that selective extraction of lead and zinc from EAF dust is possible using two methods (temperatures provided without considering the addition of inert gas to the system):

– consecutive reduction of lead containing phases (295 – 877 °C) and zinc containing phases (794 – 1326 °C) by carbon or carbon monoxide;

– reduction of lead-containing phases (295 – 877 °C) by carbon or carbon monoxide, followed by the thermal dissociation of zinc-containing phases (1970 °C).

The need to investigate the mechanism of consecutive reduction of lead-containing phases and zinc-containing phases from EAF dust is driven by the preference for operating the process at lower temperatures. This would result in reduced energy consumption and the ability to carry out the process without the formation of a melt.

However, the temperatures in the actual process may deviate significantly from the calculated values. In order to determine the actual temperatures for the selective extraction of lead and zinc from EAF dust, an experimental study was conducted.

Experimental

The experimental study involved heating EAF dust in the temperature range of 20 – 1300 °C using a vacuum

Table 3

Franklinite reduction chemical reactions and their course temperatures

Таблица 3. **Химические реакции восстановления франклинита и температуры их протекания**

No.	Reaction	Reaction temperature, °C
10	$ZnFe_2O_4 + CO_{(g)} = ZnO + 2FeO + CO_{2(g)}$	>838
11	$ZnFe_2O_4 + 4C = Zn_{(g)} + 2Fe + 4CO_{(g)}$	>794
12	$ZnFe_2O_4 + 2C = Zn_{(g)} + 2Fe + 2CO_{2(g)}$	>863
13	$ZnFe_2O_4 + 3CO_{(g)} = ZnO + 2Fe + 3CO_{2(g)} + ZnO + CO_{(g)} = Zn_{(g)} + CO_{2(g)} = \sum ZnFe_2O_4 + 2CO_{(g)} = Zn_{(g)} + 2FeO + 2CO_{2(g)}$	>1126
14	$ZnFe_2O_4 + CO_{(g)} = ZnO + 2FeO + CO_{2(g)} + ZnO + C = Zn_{(g)} + CO_{(g)} = \sum ZnFe_2O_4 + C = Zn_{(g)} + 2FeO + CO_{2(g)}$	>905

Table 4

Fe_3O_4 and Mn_3O_4 reduction chemical reactions and their course temperatures

Таблица 4. **Химические реакции восстановления оксидов Fe_3O_4 и Mn_3O_4 и температуры их протекания**

No.	Reaction	Reaction temperature, °C
15	$Fe_3O_4 + C = 3FeO + CO_{(g)}$	>700
16	$2Fe_3O_4 + C = 6FeO + CO_{2(g)}$	>694
17	$Fe_3O_4 + CO_{(g)} = 3FeO + CO_{2(g)}$	>514
18	$FeO + C = Fe + CO_{(g)}$	>725
19	$2FeO + C = 2Fe + CO_{2(g)}$	>751
20	$FeO + CO_{(g)} = Fe + CO_{2(g)}$	<579
21	$Fe_3O_4 + C = Fe_2O_3 + Fe + CO_{(g)}$	>941
22	$Mn_3O_4 + C = 3MnO + CO_{(g)}$	>277
23	$2Mn_3O_4 + C = 6MnO + CO_{2(g)}$	0 – 2000
24	$Mn_3O_4 + CO_{(g)} = 3MnO + CO_{2(g)}$	0 – 2000
25	$MnO + C = Mn + CO_{(g)}$	>1397

Table 5

Zinc oxide thermal dissociation chemical reaction and its course temperature

Таблица 5. **Химическая реакция термической диссоциации оксида цинка и температура ее протекания**

No.	Reaction	Reaction temperature, °C
26	$2ZnO = 2Zn_{(g)} + O_{2(g)}$	>2118

resistance furnace with constant heating rate and a Tamman furnace under isothermal conditions with argon flow. Prior to the study, a blank test was conducted to ensure that the weight loss of the crucible did not affect the measurements of the sample weight.

The temperature in the furnace was monitored using BP(A) 5/20 thermocouple placed in the isothermal area of the furnace, inside an empty crucible.

After the samples were cooled, they were weighed and subjected to chemical composition analysis.

The carbon and sulfur content in the samples was determined using a Leco CS 600 instrument through high temperature extraction in a gas carrier. The element content from Na to U was determined using a MAX-GVM wave-dispersion *X*-ray fluorescent spectroscan (MAX-GVM).

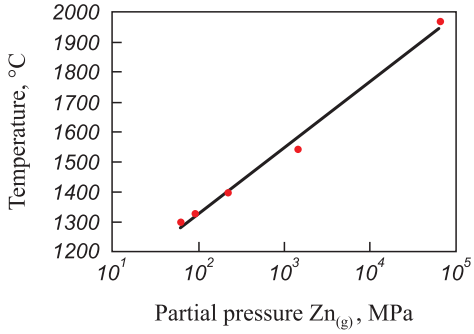

Fig. 1. Dependence of $ZnO = Zn_{(g)} + O_{2(g)}$ reaction temperature on $Zn_{(g)}$ partial pressure

Рис. 1. Зависимость температуры протекания реакции $ZnO = Zn_{(r)} + O_{2(r)}$ от парциального давления $Zn_{(r)}$

Experiments in a vacuum resistance furnace

EAF dust from bag filters was subjected to processing in a vacuum resistance furnace (Fig. 2) equipped with a graphite heater (D = 65 mm, L = 300 mm) in the temperature range of 20 – 1300 °C. The furnace specification are as follows: P = 20 kW; U = 10 V; I = 2000 A; f = 50 Hz. The furnace is equipped with a water cooling system.

A total of 3 g of the dust was placed in a thin-walled alundum crucible (D = 19 mm, d = 18 mm, H = 40 mm, h = 38.5 mm). The layer height was maintained at 1.25 – 1.5 cm. Seven crucibles, weighting a dust total of 21 g, were placed in the isothermal area of the furnace. From the furnace chamber was evacuated air using a vacuum pump to reach a residual pressure of 10^{-1} Pa, after which it was filled with high-purity argon.

Subsequently, the gas was discharged into the atmosphere and the argon flow rate was set to 0.5 l/min. The furnace was heated at a rate of 15 °C/min, with the temperature reaching 100 °C in ~7 min. Once the desired temperature (800, 1000, 1100, 1200, 1300 °C) was reached, one to two crucibles containing the melted products were removed from the furnace and cooled in ambient air.

The appearance of the samples before and after processing in the furnace is depicted in Fig. 3. After heating, the samples exhibited a darkened color, likely due to partial reduction of magnetite. The samples processed at 800 and 1000 °C crumbled under light pressure, while those processed at 1100 and 1200 °C were easily milled in mortar. Heating to 1300 °C resulted in the formation of a melt.

After cooling, the samples were analyzed to determine their chemical composition. The actual weight loss of the samples after heating is presented in Table 6, showing a significant increase in weight loss at 1200 °C and higher temperatures.

The contents of lead, zinc (determined using a MAX-GVM wave-dispersion *X*-ray fluorescent spectroscan), and car-

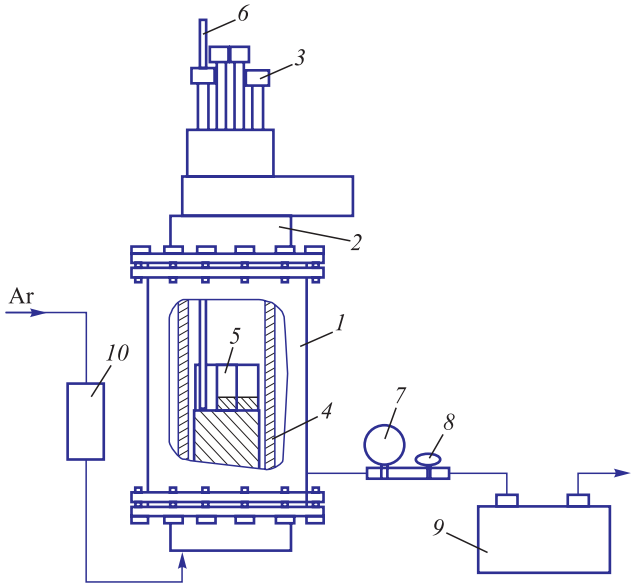

Fig. 2. Scheme of vacuum resistance furnace:
1 – furnace body; *2* – furnace lid; *3* – observation hole; *4* – graphite heater; *5* – working alund crucibles; *6* – BP 5/20 thermocouple; *7* – monometer; *8* – vacuum system valve; *9* – vacuum pump; *10* – rotameter

Рис. 2. Схема вакуумной печи сопротивления:
1 – корпус печи; *2* – крышка печи; *3* – смотровое окно; *4* – графитовый нагреватель; *5* – рабочие алундовые тигли; *6* – термопара ВР 5/20; *7* – манометр; *8* – вентиль вакуумной системы; *9* – вакуумный насос; *10* – ротаметр

bon (determined using a Leco CS 600 instrument by high temperature extraction in a carrier gas) in the EAF dust after heating in vacuum resistance furnace in argon flow are summarized in Table 7. The extraction rate of elements as a function of processing temperature of EAF dust in the vacuum resistance furnace is illustrated in Fig. 4.

According to Fig. 4, heating the EAF dust with a constant rate at flowing argon resulted in a significant decrease in carbon, zinc, and lead content. The removal of lead and zinc from the sample occurred in the temperature range of 800 – 1200 °C, with a higher extraction rate observed for lead. The intensive removal of lead occurred at temperatures above 1000 °C, while the intensive removal of zinc started at the temperatures above 1100 °C. To further investigate the possibility of selectively removing lead and zinc from EAF dust, their behavior in the temperature range of 800 – 1200 °C needs to be studied under isothermal conditions using the Tamman furnace, allowing for similar experiments to be conducted.

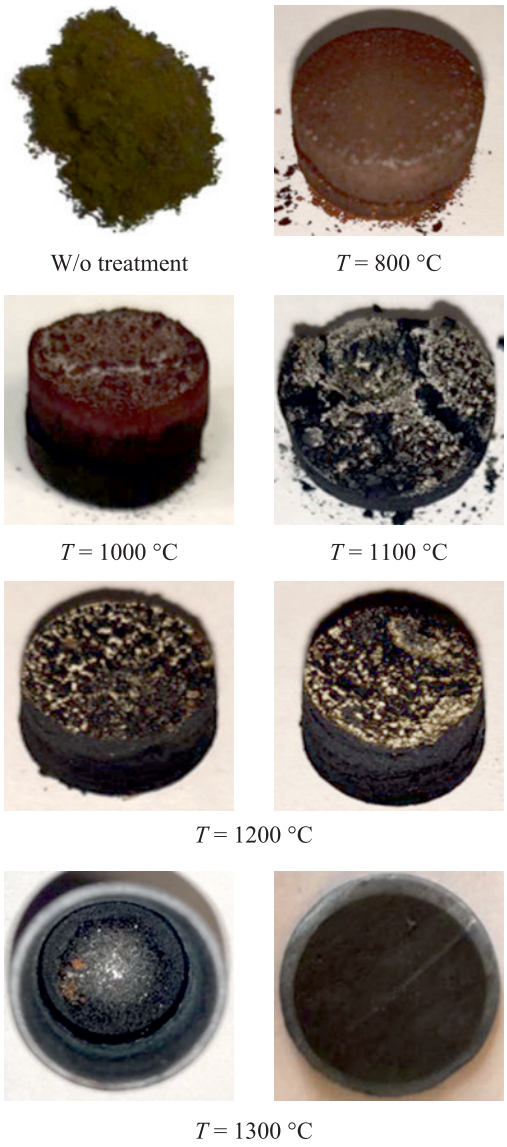

Fig. 3. Appearance of the samples before and after treatment in the vacuum resistance furnace

Рис. 3. Внешний вид образцов до и после обработки в вакуумной печи сопротивления

Table 6

Actual EAF dust mass decrease after heating in the vacuum resistance furnace with flowing argon

Таблица 6. **Фактическая убыль массы навески пыли ДСП после нагрева в вакуумной печи сопротивления в токе аргона**

Holding temperature, °C	Actual mass decrease, rel. %
800	2.32
1000	3.64
1100	4.28
1200	10.04*
1300	21.49*

* Averaged by two samples.

Experiments in a Tamman furnace

EAF dust from bag filters of the gas scrubbing system was subjected to processing in a Tamman furnace with a graphite heater (D = 80 mm, L = 400 mm) in the tem-

Table 7

Lead, zinc and carbon content in EAF dust before and after heating in the vacuum resistance furnace with flowing argon

Таблица 7. **Содержание свинца, цинка и углерода в пыли ДСП до и после нагрева в вакуумной печи сопротивления в токе аргона**

Element	Initial composition	Content of elements (wt. %) at the temperature of treatment, °C						
		800	1000	1100	1200		1300	
C	1.74	1.29	0.92	0.40	0.06	0.06	n.a.	n.a.
Zn	14.50	14.70	14.80	14.70	9.40	9.70	7.90	8.40
Pb	1.00	1.00	0.70	0.60	0	0	0	0

R e m a r k: n.a. – not available.

perature range of 800 – 1200 °C, with holding time: 3, 6, 9, 12 min. The furnace specifications are as follows: $P = 40$ kW; $f = 50$ Hz. The flowing argon rate (high purity) was set to 1 l/min. The furnace is equipped with a water cooling system.

A total of 3 g of EAF dust was placed in a thin-walled alund crucible ($D = 19$ mm, $d = 18$ mm, $H = 40$ mm, $h = 38.5$ mm), with a layer height of 1.25 – 1.50 cm.

Once the preset temperature in the furnace chamber was reached (800, 900, 1000, 1100, 1200 °C), four samples arranged in a cartridge were simultaneously placed into the furnace. The time of sample placement into the furnace was considered as the starting time of the experiment. The samples at each temperature were held for 3, 6, 9, 12 min.

As the furnace temperature and holding time increased, the color of samples varies from brown, dark brown and dark grey to black, which is likely attributed to the partial reduction of magnetite. The samples held at 800, 900, 1000 and 1100 °C (for no longer than for three minutes) retained their shapes but crumbled under light pressure. The samples held at 1100 °C for three minutes, upon extraction from the crucible, retained their shape under pressure, but could be easily milled in a mortar. The samples held at 1200 °C required considerable force to be milled in a mortar. Meanwhile, the samples held at 1200 °C for more than 6 min were difficult to extract from the crucible.

After cooling in ambient air, the samples were weighed, and their chemical composition was analyzed by the aforementioned methods. The actual weight loss of the samples after heating in the amman furnace with flowing argon is presented in Table 8, with a significantly higher weight loss observed at 1200 °C.

The contents of lead, zinc (determined using a MAX-GVM wave-dispersion *X*-ray fluorescent spectroscan), and carbon (determined using a Leco CS 600 instrument by high temperature extraction in a carrier gas) in the EAF dust after heating in the Tamman furnace with flowing argon are summarized in Table 9.

The extraction rates of carbon, zinc, and lead from EAF dust as a function of holding time during heating in the Tamman furnace (800 – 200 °C) with flowing argon are illustrated in Figs. 5 – 7.

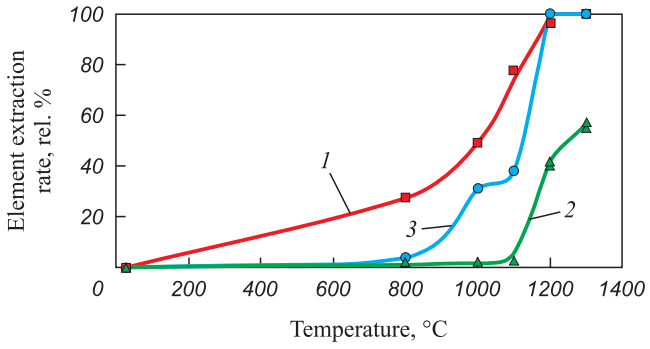

Fig. 4. Dependence of the element extraction rate on the temperature of EAF dust treatment in vacuum resistance furnace:
1 – C; *2* – Zn; *3* – Pb

Рис. 4. Зависимость степени извлечения элемента от температуры обработки пыли ДСП в вакуумной печи сопротивления:
1 – C; *2* – Zn; *3* – Pb

Table 8

Actual EAF dust mass decrease after heating and holding in the Tamman furnace with flowing argon

Таблица 8. **Фактическая убыль массы навески пыли ДСП после нагрева и выдержки в печи Таммана в токе аргона**

Holding temperature of samples, °C	Actual mass decrease, rel. %, at holding time, min			
	3	6	9	12
800	0.67	1.67	2.67	4.00
900	1.00	2.33	3.33	4.33
1000	1.67	2.67	4.00	5.33
1100	2.33	3.67	5.67	6.67
1200	8.67	10.33	12.33	14.00

According to Figs. 5 – 7, during the isothermal heating of EAF dust in an inert environment, the concentrations of lead, zinc and carbon underwent changes.

Complete transition of lead into the gas phase during the experiments was achieved at 1100 °C (holding time: 12 min) and at 1200 °C (holding time: 6 min and higher). However, at 900 and 1000 °C, increasing the holding time from 9 to 12 min did not result in an increased extraction rate of lead when carbon was present in the samples. This suggests that there may be a combined process involving multiple reactions of Pb_2O_3 reduction within the temperature range of 800 – 1200 °C.

Simultaneously with the transition of lead into the gas phase, there was an extraction of zinc, amounting of 14.4 % (relative) (t = 1100 °C, holding time: 12 min) and 32.2 % (relative) (t = 1200 °C, holding time: 6 min and longer), respectively. This indicates a failure to achieve selective extraction of lead during the heating of EAF dust under the experimental conditions. Further heating of the EAF dust would likely lead to selective extraction of zinc, as it appears that lead was completely removed from the EAF dust during the experiment. It is possible to achieve higher selectivity in the extraction of zinc and lead by adjusting the process temperatures for specific dust compositions. At 1200 °C, the extraction rate of zinc reaches a plateau, while the carbon content in the EAF dust decreases to zero. This suggests that the reduction reactions of zinc-containing phases ceased due to an insufficient amount of reducing agent.

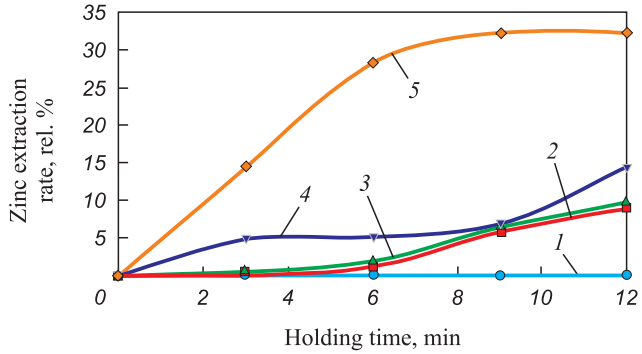

Fig. 7. Dependence of the extraction rate of zinc from EAF dust on the holding time during heating in the Tamman furnace with flowing argon at, °C:
1 – 800; *2* – 900; *3* – 1000; *4* – 1100; *5* – 1200

Рис. 7. Зависимость степени извлечения цинка из пыли ДСП от времени выдержки при нагреве в печи Таммана в токе аргона, °C:
1 – 800; *2* – 900; *3* – 1000; *4* – 1100; *5* – 1200

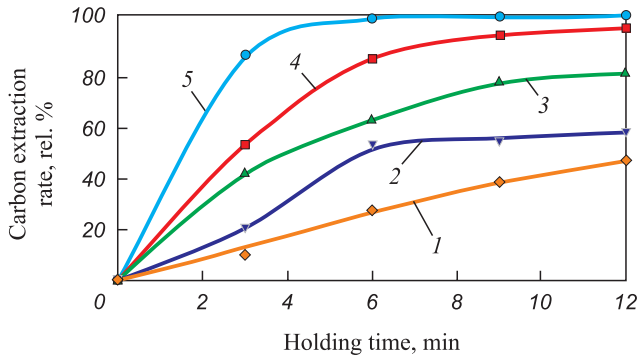

Fig. 5. Dependence of the extraction rate of carbon from EAF dust on the holding time during heating in the Tamman furnace with flowing argon at, °C:
1 – 800; *2* – 900; *3* – 1000; *4* – 1100; *5* – 1200

Рис. 5. Зависимость степени извлечения углерода из пыли ДСП от времени выдержки при нагреве в печи Таммана в токе аргона, °C:
1 – 800; *2* – 900; *3* – 1000; *4* – 1100; *5* – 1200

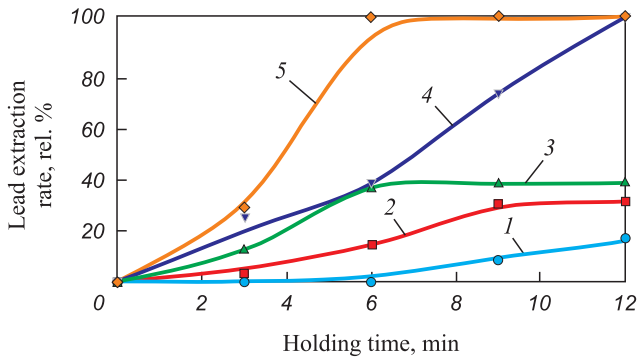

Fig. 6. Dependence of the extraction rate of lead from EAF dust on the holding time during heating in the Tamman furnace with flowing argon at, °C:
1 – 800; *2* – 900; *3* – 1000; *4* – 1100; *5* – 1200

Рис. 6. Зависимость степени извлечения свинца из пыли ДСП от времени выдержки при нагреве в печи Таммана в токе аргона, °C:
1 – 800; *2* – 900; *3* – 1000; *4* – 1100; *5* – 1200

Comparison of the experimental data with the results of thermodynamical simulation in HSC Chemistry 6 software confirmed that the transition of lead-containing phases of EAF dust into the gas state can occur according to reactions 1 – 6 (see Table 1). Furthermore, the transition of zinc-containing phases of EAF dust into the gas state most likely occurs through reactions 7 – 8 (see Table 2) and 12 – 14 (see Table 3).

The carbon content present in the EAF dust was not sufficient for the complete recovery of zinc from its compounds, particularly due to the presence of manganese and iron in the complex spinel composition $(Zn, Mn, Fe)_3O_4$. In order to achieve the full recovery of zinc-containing phases in the dust sample, the addition of a reducing agent in the form of carbon or CO is required. Since an additional reducing agent is needed after the recovery of the lead-containing phase, the most effective approach appears to be the intensification of zinc recovery from the electric arc furnace dust by CO purging. Increasing the flow rate of the reducing agent allows for a reduction in the recovery temperature of zinc [21]. For example, increasing the CO concentration from 75 to 85 % at 1200 °C results in four-five times increase in the intensity of zinc removal to the gas phase [13].

Table 9

Lead, zinc and carbon content change in EAF dust after heating and holding in the Tamman furnace with flowing argon

Таблица 9. **Изменение содержания свинца, цинка и углерода в пыли ДСП после нагрева и выдержки в печи Таммана в токе аргона**

Element	Temperature of treatment, °C	Initial composition, wt. %	Chemical composition of dust, wt. % at holding time, min			
			3	6	9	12
C	800	1.74	1.59	1.31	1.13	1.00
Zn		14.50	14.60	14.70	14.90	15.00
Pb		1.00	1.00	1.00	0.90	0.90
C	900	1.74	1.41	0.87	0.86	0.81
Zn		14.50	14.60	14.70	14.20	13.80
Pb		1.00	1.00	0.90	0.70	0.70
C	1000	1.74	1.06	0.71	0.47	0.41
Zn		14.50	14.70	14.60	14.10	13.80
Pb		1.00	0.90	0.60	0.60	0.60
C	1100	1.74	0.88	0.30	0.15	0.10
Zn		14.50	14.10	14.30	14.30	13.30
Pb		1.00	0.70	0.60	0.30	0
C	1200	1.74	0.29	0.04	0.02	0.01
Zn		14.50	13.60	11.60	11.20	11.40
Pb		1.00	0.80	0	0	0

Researchers [22] have conducted studies on the recovery of zinc and iron from EAF dust using carbon monoxide as a reducing agent at various temperatures within the pyrometallurgical process. The optimal working temperature was found to be 950 °C. However, they also observed the negative influence of other impurities such as alkali-metal chlorides (NaCl, KCl) and lead compounds. The impact of these impurities can be mitigated by implementing a selective extraction process for lead and zinc from the EAF dust.

Conclusions

Thermodynamic simulation was performed to investigate the selective extraction of zinc and lead from EAF dust. Two methods were determined to achieve selective extraction (the temperatures are given without accounting for addition of an inert gas into the system):

– consecutive recovery of lead-containing (295 – 877 °C) and zinc-containing (794 – 1326 °C) phases using carbon or carbon monoxide;

– recovery of lead-containing phases (295 – 877 °C) using carbon or carbon monoxide, followed by thermal dissociation of zinc-containing phases (1970 °C).

Experimental studies conducted in the vacuum resistance furnace with linear heating revealed that the removal of lead and zinc occurred within the temperature range of 800 – 1200 °C. The rate of lead removal was higher, with intensive removal observed at temperature above 1000 °C, while zinc removal was more pronounced at temperature above 1200 °C.

Additional corrective isothermal experiments carried out in the Tamman furnace showed that complete transfer of lead into the gas phase was achieved at 1100 °C (holding time: 12 min) and at 1200 °C (holding time: 6 min and longer). However, during this transition, the extraction of lead was only 14.4 and 32.2 rel. %, respectively, indicating a failure to achieve selective lead extraction during the heating of EAF dust in the experiments. It is expected that further heating of the EAF dust would lead to selective zinc extraction, as the lead has been completely removed.

A comparison between the experimental data and the results of thermodynamic simulation allowed the identification of the most probable reactions involved in the recovery of lead and zinc containing phases.

References / Список литературы

1. Patrushov A.E. Technical and economic efficiency evaluation of pyrometallurgical technology for processing dust from electric steel production. *iPolytech Journal*. 2020;24(3): 672–683. (In Russ.).
https://doi.org/10.21285/1814-3520-2020-3-672-683

Патрушов А.Е. Оценка технико-экономической эффективности пирометаллургической технологии переработки пылей электросталеплавильного производства. *Вестник Иркутского государственного технического университета*. 2020;24(3):672–683.
http://dx.doi.org/10.21285/1814-3520-2020-3-672-683

2. Tyushnyakov S.N., Selivanov E.N., Pankratov A.A. Forms of zinc found in electric steel smelting furnace gas cleaning dust. *Metallurgist*. 2018;62(5-6):485–492.
https://doi.org/10.1007/s11015-018-0685-z

Тюшняков С.Н., Селиванов Е.Н., Панкратов А.А. Формы нахождения цинка в пыли газоочистки электросталеплавильных печей. *Металлург*. 2018;(6):8–13.

3. Da Silva Machado J.G.M., Brehm F.A., Moraes C.A.M., dos Santos C.A., Vilela A.C.F. Characterization study of electric arc furnace dust phases. *Materials Research*. 2006;9(1):30–36.
https://doi.org/10.1590/S1516-14392006000100009

4. Ahmad S., Sajal W.R., Gulshan F., Hasan M., Rhamdhani M.A. Thermodynamic analysis of caustic–roasting of electric arc furnace dust. *Heliyon*. 2022;8(10):e11031.
https://doi.org/10.1016/j.heliyon.2022.e11031

5. Omran M., Fabritius T. Effect of steelmaking dust characteristics on suitable recycling process determining: Ferrochrome converter (CRC) and electric arc furnace (EAF) dusts. *Powder Technology*. 2017;308:47–60.
http://dx.doi.org/10.1016/j.powtec.2016.11.049

6. Halli P., Agarwal V., Partinen J., Lundström M. Recovery of Pb and Zn from a citrate leach liquor of a roasted EAF dust using precipitation and solvent extraction. *Separation and Purification Technology*. 2020;236:116264.
https://doi.org/10.1016/j.seppur.2019.116264

7. Leclerc N., Meux E., Lecuire J.-M. Hydrometallurgical recovery of zinc and lead from electric arc furnace dust using mononitrilotriacetate anion and hexahydrated ferric chloride. *Journal of Hazardous Materials*. 2001;91(1–3):257–270.
https://doi.org/10.1016/S0304-3894(01)00394-6

8. Antuñano N., Cambra J.F., Arias P.L. Hydrometallurgical processes for Waelz oxide valorisation – An overview. *Process Safety and Environmental Protection*. 2019;129:308–320.
https://doi.org/10.1016/j.psep.2019.06.028

9. Al-Harahsheh M., Altarawneh S., Al-Omari M. Selective dissolution of zinc and lead from electric arc furnace dust via oxidative thermolysis with polyvinyl chloride and water-leaching process. *Hydrometallurgy*. 2022;212:105898.
https://doi.org/10.1016/j.hydromet.2022.105898

10. Razinkova O.A. Sources of environmental pollution in hydrometallurgical production and ways of their use. *Nauchnyi potentsial regionov na sluzhbu modernizatsii*. 2013;(1):25–29. (In Russ.).

Разинкова О.А. Источники загрязнения окружающей среды в гидрометаллургическом производстве и пути их использования. *Научный потенциал регионов на службу модернизации*. 2013;(1):25–29.

11. Wang L., Peng Z., Lin X., Ye Q., Ye L., Zhang J., Liu Y., Liu M., Rao M., Li G., Jiang T. Microwave-intensified treatment of low-zinc EAF dust: A route toward high-grade metallized product with a focus on multiple elements. *Powder Technology*. 2021;383:509–521.
https://doi.org/10.1016/j.powtec.2021.01.047

12. Adedoyin F.F., Gumede M.I., Bekum F.V., Etokakpan M.U., Balsalobre-Lorente D. Modelling coal rent, economic growth and CO_2 emissions: Does regulatory quality matter in BRICS economies? *Science of the Total Environment.* 2020;710:136284.
https://doi.org/10.1016/j.scitotenv.2019.136284

13. Marchenko N.V., Vershinina E.P., Gil'debrandt E.M. *Metallurgy of Heavy Non-Ferrous Metals*. Available at URL: https://c-metal.ru/image/catalog/books/Marchenko.pdf (Accessed 11.05.2023). (In Russ.).

Марченко Н.В., Вершинина Е.П., Гильдебрандт Э.М. *Металлургия тяжелых цветных металлов: Электронное учебное пособие* [Электронный ресурс]. Красноярск: ИПК СФУ, 2009. URL: https://c-metal.ru/image/catalog/books/Marchenko.pdf (дата обращения 11.05.2023).

14. Simonyan L.M., Demidova N.V. Selective extraction of carbon-free zinc and lead from EAF-dust. *Izvestiya. Ferrous Metallurgy*. 2020;63(8):631–638. (In Russ.).
https://doi.org/10.17073/0368-0797-2020-8-631-638

Симонян Л.М., Демидова Н.В. Исследование процесса безуглеродного селективного извлечения цинка и свинца из пыли ДСП. *Известия вузов. Черная металлургия*. 2020;63(8):631–638.
https://doi.org/10.17073/0368-0797-2020-8-631-638

15. Grudinsky P.I., Dyubanov V.G., Kozlov P.A. Distillation separation of the copper-smelting dusts with primary recovery of lead. *Russian Metallurgy(Metally)*. 2018;2018(1):7–13.
https://doi.org/10.1134/S003602951801007X

Грудинский П.И., Дюбанов В.Г., Козлов П.А. Исследование процессов дистилляционного разделения пыли плавки меди с первичным извлечением свинца. *Металлы*. 2018;(1):9–16.

16. Jabbour K., El Hassan N. Optimized conditions for reduction of iron (III) oxide into metallic form under hydrogen atmosphere: A thermodynamic approach. *Chemical Engineering Science*. 2022;252:117297.
https://doi.org/10.1016/j.ces.2021.117297

17. Kleonovskii M.V., Sheshukov O.Yu., Mikheenkov M.A., Lozovaya E.Yu. Thermodynamic modeling of zinc recovery from ferrous metallurgy sludge. *Izvestiya. Ferrous Metallurgy*. 2022;65(3):170–178. (In Russ.).
https://doi.org/10.17073/0368-0797-2022-3-170-178

Клеоновский М.В., Шешуков О.Ю., Михеенков М.А., Лозовая Е.Ю. Термодинамическое моделирование восстановления цинка из шламов черной металлургии. *Известия вузов. Черная металлургия*. 2022;65(3):170–178.
https://doi.org/10.17073/0368-0797-2022-3-170-178

18. Omran M., Fabritius T. Utilization of blast furnace sludge for the removal of zinc from steelmaking dusts using microwave heating. *Separation and Purification Technology*. 2019;210:867–884.
https://doi.org/10.1016/j.seppur.2018.09.010

19. Li C., Liu W., Jiao F., Yang C., Li G., Liu S., Qin W. Separation and recovery of zinc, lead and iron from electric arc furnace dust by low temperature smelting. *Separation and Purification Technology*. 2023;312:123355.
https://doi.org/10.1016/j.seppur.2023.123355

20. Trusov B.G. TERRA software system for modeling phase and chemical equilibria. In: *Abstracts of the XIV Int. Conf. on Chemical Thermodynamics*. St. Petersburg: NII Chimii SpbSU; 2002:483. (In Russ.).

Трусов Б.Г. Программная система TERRA для моделирования фазовых и химических равновесий. *Тезисы докладов XIV Международной конференции по химической термодинамике*. СПб: НИИ Химии СПбГУ; 2002:483.

21. Vusikhis A.S., Selivanov E.N., Leont'ev L.I., Tyushnyakov S.N. Thermodynamic simulation of metal reduction from B_2O_3–CaO–FeO–ZnO melts by hydrogen and carbon monoxide. *Russian Metallurgy (Metally)*. 2022;2022(5): 475–480. https://doi.org/10.1134/S0036029522050111

Вусихис А.С., Селиванов Е.Н., Леонтьев Л.И., Тюшняков С.Н. Термодинамическое моделирование процессов восстановления металлов из расплавов B_2O_3–CaO–FeO–ZnO. *Металлы*. 2022;(3):17–23.

22. Wu C.-C., Chang F.-C., Chen W.-S., Tsay M.-S., Wang Y.-N. Reduction behavior of zinc ferrite in EAF-dust recycling with CO gas as a reducing agent. *Journal of Environmental Management*. 2014;143:208–213. https://doi.org/10.1016/j.jenvman.2014.04.005

Information about the Authors

Nadezhda V. Podusovskaya, *Junior Researcher of the Laboratory of Materials Diagnostics,* Baikov Institute of Metallurgy and Materials Science, Russian Academy of Sciences; *Postgraduate of the Chair of Metallurgy of Steel, New Production Technologies and Metal Protection,* National University of Science and Technology "MISIS"
ORCID: 0000-0002-4124-0444
E-mail: ndemidova_n@mail.ru

Ol'ga A. Komolova, *Cand. Sci. (Eng.), Senior Researcher of the Laboratory of Materials Diagnostics,* Baikov Institute of Metallurgy and Materials Science, Russian Academy of Sciences; *Assist. Prof. of the Chair of Metallurgy of Steel, New Production Technologies and Metal Protection*, National University of Science and Technology "MISIS"
ORCID: 0000-0001-9517-8263
E-mail: o.a.komolova@gmail.com

Konstantin V. Grigorovich, *Academician, Dr. Sci. (Eng.), Head of the Laboratory of Materials Diagnostics,* Baikov Institute of Metallurgy and Materials Science, Russian Academy of Sciences; *Prof. of the Chair of Metallurgy of Steel, New Production Technologies and Metal Protection,* National University of Science and Technology "MISIS"
ORCID: 0000-0002-5669-4262
E-mail: grigorov@imet.ac.ru

Aleksandr V. Pavlov, *Dr. Sci. (Eng.), Prof. of the Chair of Metallurgy of Steel, New Production Technologies and Metal Protection,* National University of Science and Technology "MISIS"
ORCID: 0000-0003-3773-9469
E-mail: pav-gnts@misis.ru

Viktoriya V. Aksenova, *Postgraduate of the Chair of Metallurgy of Steel, New Production Technologies and Metal Protection,* National University of Science and Technology "MISIS"
E-mail: axenovaviki@gmail.com

Boris A. Rumyantsev, *Cand. Sci. (Eng.), Research Associate of the Laboratory of Materials Diagnostics,* Baikov Institute of Metallurgy and Materials Science, Russian Academy of Sciences
ORCID: 0000-0001-8250-3565
E-mail: brumyantsev@imet.ac.ru

Mark V. Zheleznyi, *Junior Researcher of the Laboratory of Materials Diagnostics,* Baikov Institute of Metallurgy and Materials Science, Russian Academy of Sciences; *Assistant of the Chair of Physical Materials,* National University of Science and Technology "MISIS"
ORCID: 0000-0003-3821-6790
E-mail: markiron@mail.ru

Сведения об авторах

Надежда Владимировна Подусовская, *младший научный сотрудник лаборатории диагностики материалов,* Институт металлургии и материаловедения им. А.А. Байкова РАН; *аспирант кафедры металлургии стали, новых производственных технологий и защиты металлов*, Национальный исследовательский технологический университет «МИСИС»
ORCID: 0000-0002-4124-0444
E-mail: ndemidova_n@mail.ru

Ольга Александровна Комолова, *к.т.н., старший научный сотрудник лаборатории диагностики материалов,* Институт металлургии и материаловедения им. А.А. Байкова РАН; *доцент кафедры металлургии стали, новых производственных технологий и защиты металлов*, Национальный исследовательский технологический университет «МИСИС»
ORCID: 0000-0001-9517-8263
E-mail: o.a.komolova@gmail.com

Константин Всеволодович Григорович, *академик РАН, д.т.н., заведующий лабораторией диагностики материалов,* Институт металлургии и материаловедения им. А.А. Байкова РАН; *профессор кафедры металлургии стали, новых производственных технологий и защиты металлов*, Национальный исследовательский технологический университет «МИСИС»
ORCID: 0000-0002-5669-4262
E-mail: grigorov@imet.ac.ru

Александр Васильевич Павлов, *д.т.н., профессор кафедры металлургии стали, новых производственных технологий и защиты металлов*, Национальный исследовательский технологический университет «МИСИС»
ORCID: 0000-0003-3773-9469
E-mail: pav-gnts@misis.ru

Виктория Владимировна Аксенова, *аспирант кафедры металлургии стали, новых производственных технологий и защиты металлов*, Национальный исследовательский технологический университет «МИСИС»
E-mail: axenovaviki@gmail.com

Борис Алексеевич Румянцев, *к.т.н., научный сотрудник лаборатории диагностики материалов,* Институт металлургии и материаловедения им. А.А. Байкова РАН
ORCID: 0000-0001-8250-3565
E-mail: brumyantsev@imet.ac.ru

Марк Владимирович Железный, *младший научный сотрудник лаборатории диагностики материалов,* Институт металлургии и материаловедения им. А.А. Байкова РАН; *ассистент кафедры физического материаловедения*, Национальный исследовательский технологический университет «МИСИС»
ORCID: 0000-0003-3821-6790
E-mail: markiron@mail.ru

Contribution of the Authors / Вклад авторов

N. V. Podusovskaya – conducting thermodynamic calculations, planning and conducting experiments, processing of the obtained experimental data, writing the text.
O. A. Komolova – setting the research goal, experiments planning, discussion of the results and conclusions.
K. V. Grigorovich – setting the research goal, formation of the article main concept, discussion of the results and conclusions.
A. V. Pavlov – planning and organization of experiments.
V. V. Aksenova – samples chemical composition determination by wave-dispersive X-ray fluorescence spectroscopy (MAX-GVM).

B. A. Rumyantsev – determination of S and C content by high-temperature extraction in a carrier gas (Leco CS 600).

M. V. Zheleznyi – X-ray diffraction analysis (XRD) of initial dust composition.

Н. В. Подусовская – проведение термодинамических расчетов, планирование и проведение экспериментов, обработка полученных экспериментальных данных, подготовка текста статьи.
О. А. Комолова – определение цели работы, планирование экспериментов, обсуждение результатов и выводов.
К. В. Григорович – определение цели работы и общей концепции статьи, обсуждение результатов и выводов.
А. В. Павлов – планирование и организация экспериментов.
В. В. Аксенова – определение химического состава образцов методом волно-дисперсионной рентгенофлуоресцентной спектроскопии (МАКС-GVM).
Б. А. Румянцев – определение содержания в образцах серы и углерода методом высокотемпературной экстракции в несущем газе (Leco CS 600).
М. В. Железный – проведение рентгенодифракционного анализа (XRD) исходного состава пыли.

Received 03.05.2023
Revised 05.05.2023
Accepted 05.05.2023

Поступила в редакцию 03.05.2023
После доработки 05.05.2023
Принята к публикации 05.05.2023